10-Hydroxydec-2-enoic acid enhances the erythrocyte membrane fluidity via interacting with phosphatidylcholine and phosphatidylethanolamine

Fangfang Sha[1], Peichang Yang[1], Hui Wang[2], Junhua Ren[1,2], Zirui Li[1], Lu Zhang[1]*, Pei Fan[1]*

[1]School of Biological Engineering, Henan University of Technology, 450001 Zhengzhou, China; [2]Institute of Tropical Bioscience and Biotechnology, Chinese Academy of Tropical Agricultural Sciences, 571101 Haikou, China

***Corresponding Authors:** Lu Zhang and Pei Fan, No. 100, Lianhua Street, School of Biological Engineering, Henan University of Technology, Zhengzhou, 450001, China. Emails: zhanglu@haut.edu.cn and apisfp@126.com

Received: 20 April 2023; Accepted: 20 November 2023; Published 7 December 2023

OPEN ACCESS

SHORT COMMUNICATION

Abstract

10-Hydroxydec-2-enoic acid (10-HDA), the unique substance in the natural food royal jelly, is an unsaturated hydroxyl fatty acid with the bio-activity to guard against cell or tissue damages. However, the relevant mechanisms still remain largely unknown. Here, using a mouse erythrocyte model, whether the fluidity of plasma membrane is influenced by 10-HDA was investigated. 10-HDA was shown to enhance the erythrocyte membrane fluidity and to rescue the fluidity from •OH toxicity. In such occasions, 10-HDA promoted the dissolved O_2 level in erythrocyte suspension thereof. The levels of β-actin and band 4.1 protein were not affected by 10-HDA in erythrocytes. In the framework of density functional theory, 10-HDA may interact with phosphatidylcholine and phosphatidylethanolamine, the major components of membrane lipid bilayer. This was evidenced by the fact that 10-HDA was detectable in erythrocytes after its addition to the erythrocyte suspension. Moreover, the fluorescent intensity of erythrocytes stained by the membrane probe DiIC18(5) increased with 10-HDA treatment. Hence, 10-HDA could regulate the erythrocyte membrane fluidity and the release of O_2 from erythrocytes via targeting lipids rather than proteins. Our data cast light on the elucidation of the mechanism of 10-HDA modulating cell functionality and the utilization of 10-HDA in remedying the erythrocyte membrane fluidity-associated symptoms.

Keywords: 10-hydroxydec-2-enoic acid; erythrocyte; membrane; fluidity

Introduction

Royal jelly (RJ) is a traditional food for global consumption. In China, RJ is mainly sourced from the Italian bee *Apis Mellifera* L. The production of RJ from China accounts for more than 90% of the world annually. 10-Hydroxydec-2-enoic acid (10-HDA), the unsaturated hydroxyl fatty acid, is only found in RJ with the content of 1.4–2.01% (Yang *et al.*, 2017). 10-HDA has multiple bio-activities, including anti-bacterial (Fratini *et al.*, 2016), anti-inflammatory (Chen *et al.,* 2016; You *et al.,* 2020; Yang *et al.,* 2018), and anti-tumor effects (Filipič *et al.,* 2015). Nevertheless, the anti-damaging activities of 10-HDA in dermal fibroblast (Zheng *et al.,* 2013), blood–brain barrier (You *et al.,* 2019), immunoorgans (Fan *et al.,* 2020), and vascular smooth muscle cell (VSMC) (Fan *et al.,* 2022) were also documented. The mechanism of 10-HDA defending against cell or tissue impairment may be its scavenging ability of hydroxyl free radical (•OH) as we previously reported (Fan *et al.,* 2022). Still, we hypothesize that other mechanisms exist for 10-HDA to protect the cellular viability. As is well-accepted, the membrane fluidity characterizes the lipid bilayer dynamics, and is essential for the maintenance of cell functionality, such as transport regulation and biological substance diffusion (Fonseca *et al.,* 2019). However, whether 10-HDA regulates cell membrane fluidity remains unknown.

Erythrocyte, or red blood cell, is a key cell type in the circulatory system. The essential role of erythrocytes is to transport O_2 and CO_2 via flowing in the networks of arteries/arterioles, veins/venules, and capillaries. The deformability of erythrocytes, closely relevant to the plasma membrane fluidity (Ajdžanović *et al.,* 2015), is required for the blood movement, for it facilitates erythrocytes to pass through the blood vessels with tiny diameters, and the large vessels at high shear rate (Shin *et al.,* 2007). Studies have proved that the decrease of erythrocyte membrane fluidity is associated with a broad range of symptoms, such as hypertension (Tsuda *et al.,* 2001), abetalipoproteinemia (Cooper *et al.,* 1977), Crohn's disease (Aozaki 1989), and childhood psoriasis (Ferretti *et al.,* 1993). Therefore, maintaining proper fluidity of erythrocyte membrane is pivotal to the body health.

Erythrocytes are distinct from other mammalian cells, for they have no nucleus and thus no *de novo* protein synthesis. The erythrocytic functions are seldomly influenced by DNA/RNA activities thereof. Hence, erythrocytes are a good model to investigate the cell membrane properties. Here, we use mouse erythrocyte to disclose 10-HDA's role in regulating membrane fluidity, which will expand our knowledge of 10-HDA guarding against cell hypofunction.

Materials and Methods

Materials

Commercial 6% mouse erythrocytes (Catalog No. H10306) were purchased from Yuanye Bio Sci & Tech Co., Ltd., Shanghai, China. To make proper cell concentration in use (e.g., 5%, 2%, or 0.5%), the erythrocytes were precipitated and resuspended in the saline of the right volume. Other major chemicals and instruments were specified in the following sections.

Erythrocyte membrane fluidity assay

To determine the effect of 10-HDA on erythrocyte membrane fluidity, the values of generalized polarization (GP) to reflect membrane fluidity were compared between erythrocytes (the CK group) and erythrocytes with 10-HDA treatment (the 10-HDA group). The treatment method was based on our previously published data (Fan *et al.,* 2022). In brief, the erythrocytes were added by 10-HDA (Yuanye Bio Sci & Tech Co., Ltd, Shanghai, China), which was dissolved in ethanol (the final conc. of 10-HDA in erythrocyte suspension was 3 mM), for 30 min. The CK erythrocytes were supplemented with ethanol in the same volume, and the pH value was adjusted the same as the 10-HDA-added sample by HCl, for 10-HDA's capacity to reduce pH. The 5% erythrocytes of 0.5 mL of both groups were added by 1mL Laurdan (10 μM) (TargetMol Chemicals Inc., Boston, USA) to co-incubate for 15 min at 37°C with gentle shaking. The cells were spinned down at 1000 g for 5 min, then resuspended in 1 mL saline. The step was repeated once. After the third time of centrifugation, the erythrocytes were resuspended in 400 μL saline and analyzed via the Fluorescence Spectrophotometer F-7100 (Hitachi, Ltd., Tokyo, Japan). The GP value was calculated by $GP = (I_{440} - I_{490})/(I_{440} + I_{490})$, in which I_{440} and I_{490} represented the fluorescent intensities at 440 nm and 490 nm, respectively, with the excitation at 340 nm (Startek *et al.,* 2021). Furthermore, to reveal the role of 10-HDA in protecting the fluidity against •OH toxicity (•OH inhibits erythrocyte membrane fluidity [Watanabe *et al.,* 1990]), the GP values of erythrocytes (control group), erythrocytes stressed with •OH (•OH group), and those added by 10-HDA (•OH + 10-HDA group) were also assayed. For •OH intervention, Fenton reagent ($FeSO_4$•$7H_2O$ (0.1 mM) and H_2O_2 (1 mM)) were supplied to the cells. The three groups were then incubated at 37°C for 3 h. All the above experiments were performed four times (n = 4) independently.

Assay for Dissolved O_2 level of erythrocyte suspension

The dissolved O_2 levels between CK and 10-HDA-added, as well as control, •OH-damaged, and •OH + 10-HDA erythrocyte suspensions were assayed, which used 2% erythrocyte suspension (30 mL) via the AR8406 Dissolved Oxygen Analyzer (SMART SENSOR®, Dongguan, China). The 10-HDA or •OH/•OH + 10-HDA treatment strategy was the same as that in the last section. In the following parts, CK and 10-HDA groups, as well as control, •OH and •OH + 10-HDA groups were treated likewise. Six replications (n = 6) were performed for each assay.

Imaging for erythrocyte morphology and quantification for malonaldehyde (MDA)

The morphologies of 5% erythrocytes of control, •OH and •OH + 10-HDA groups were imaged under the inverted microscope (Leica Microsystems CMS GmbH, Wetzlar, Germany) with 10 × 40 magnification. Moreover, the supernatants of 5% erythrocytes of the three groups were obtained and applied for quantifying MDA levels by an MDA assay kit (Yuanye Bio Sci & Tech Co., Ltd, Shanghai, China) according to its instruction. Three independent experiments (n = 3) were performed.

Western blotting

The 5% erythrocytes (CK and 10-HDA groups, as well as control, •OH and •OH + 10-HDA groups) of 3.5 mL were

spinned down and treated by 9 mL permeabilization buffer (5mM Na_3PO_4•$12H_2O$ with 0.1 mM EDTA-Na_2 and 0.03 mM PMSF). Centrifuged at 12000 rpm for 10 min, the precipitation was added 26 μL skeleton protein extraction buffer (5mM Na_3PO_4•$12H_2O$ with 2.5% Triton X-100) for 1 h at 0°C, and denatured at 95°C for 5 min with 5 × loading buffer. The proteins underwent electrophoresis via 4% spacer gel and 8% separation gel from 60 to 120 V, and transferred to the nitrocellulose membrane under 200 mA. The following steps were similar to those in our previous work (Fan *et al.,* 2022). Here, the primary antibodies used were against β-actin (Sigma-Aldrich Corp., St Louis, USA) and band 4.1 protein (EPB41) (Proteintech Group, Inc., Rosemont, USA). Each experiment had three replications (n = 3).

Calculations for the interaction mode of 10-HDA and phosphatidylcholine (PC) or phosphatidylethanolamine (PE)

The dimer between 10-HDA anion and PC or PE (to simplify the calculation, -CH_3 represented the alkane chains) molecules was studied by density functional theory (DFT), where all molecules were optimized by the Lee-Yang-Parr gradient-corrected correlation (B3LYP) hybrid functional (Becke 1993; Lee *et al.,* 1988) method and def2-SVP (Weigend 2006) basis set with Grimme's DFT-D3(BJ) empirical dispersion correction (Grimme *et al.,* 2011) via Gaussian 09 package. Harmonic vibrational frequency was performed at the same level to guarantee no imaginary frequency in these molecules, i.e., they locate on the minima of the potential energy surface. Ethanol was regarded as the implicit solvent with the solvation model based on the density (SMD) model (Marenich *et al.,* 2009) in the above calculations. The binding energy (BE) for dimers was evaluated as BE = E(dimer) – E(10-HDA)-E(PC/PE). In addition, the BE values were calculated again in water condition but not ethanol. The quantum theory of atoms in molecules (QTAIM) (Bader 1990), the electron localization function (ELF) (Becke and Edgecombe 1990), and the reduced density gradient (RDG) (Johnson *et al.,* 2010) were further used to reveal the bonding for the two dimers, in which Multiwfn 3.8 (dev) (Lu and Chen 2012) was for calculating these quantities whose input files were extracted from Gaussian formatted checkpoint files and plotted by VMD 1.9.3 (Humphrey *et al.,* 1996).

High-performance liquid chromatography (HPLC) detection for 10-HDA in erythrocytes

10-HDA was added to 1 mL 5% erythrocytes for 5 min or 30 min, prior to the centrifugation of 5 min at 1500 rpm. The cell pellets were washed in saline and re-spinned down of 3 min at 1000 rpm. The erythrocytes were resuspended by 500 μL ethanol, followed by the lysis via the JY92-II ultrasonic cell disruptor (SCIENTZ BIOTECHNOLOGY CO., LTD., Ningbo, China). After centrifugation of 5 min at 8000 rpm, the supernatant was obtained for HPLC (ACCHROM S6000 (Acchrom Tech, Beijing, China) with the C_{18} column (5 μm, 4.6 × 250 mm) (TupLabs, Tianjin, China)) assay. Parameters were set the same as we previously reported (Fan *et al.,* 2022). Each assay was performed three times (n = 3).

Analysis for DiIC18(5) (DiD)-stained erythrocyte membrane

Hundred and twenty-five microliters of 0.5% erythrocytes (CK or 10-HDA group) was added to 800 μL DiD (a fluorescent probe that specifically stains cell membrane), which was prepared from the Cell Plasma Membrane Staining Kit with DiD (Beyotime Biotechnology, Shanghai, China), to gently shake for 10 min at 37°C. Centrifuged for 5 min at 4300 rpm, the erythrocyte pellets were diluted in 625 μL pre-heated saline (37°C) for twice. The cells were finally resuspended in 300 μL saline for fluorescent intensity analysis via CytoFLEX (Beckman Coulter, Inc., Brea, USA). To visualize the fluorescence under the laser scanning confocal microscope (LSCM) (Olympus Corporation, Tokyo, Japan), the pre-treatment was performed similarly, except for using 5% erythrocytes, and resuspended in 100 μL saline at last. The integrated density/area was measured by ImageJ. All analyses had four replications (n = 4).

Statistical analysis

All data shown were Mean ± Standard Deviation. The significance of difference between two groups was determined by student's t-test, in which $p < 0.05$ was significant.

Results

10-HDA increased the fluidity of erythrocyte membrane and the dissolved O_2 level of erythrocyte suspension but did not affect the erythrocyte protein levels

To disclose the mechanism of 10-HDA modulating cell function, the membrane fluidity of erythrocytes influenced by 10-HDA was determined. With the treatment of 10-HDA to erythrocytes, GP value was significantly lowered compared to that of the CKs ($p < 0.01$) (Figure 1A). In addition, •OH significantly enhanced the GP value ($p < 0.01$), which was significantly scaled down by 10-HDA ($p < 0.01$) (Figure 1B). The dissolved O_2 level

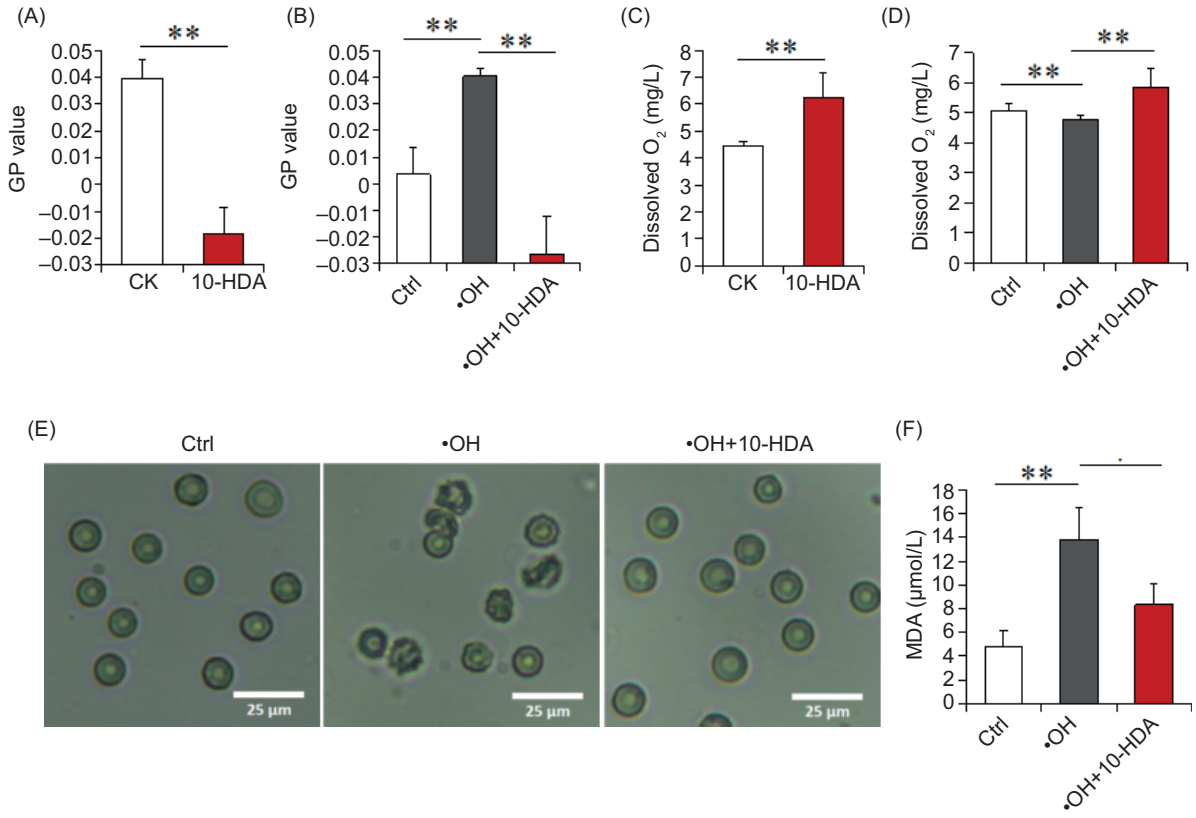

Figure 1. 10-HDA increases the erythrocyte membrane fluidity and the dissolved O_2 level of erythrocyte suspension. (A) shows the GP value variation of erythrocytes with 10-HDA addition compared to that of the CKs (n=4, $^{**}p < 0.01$). (B) represents the GP value differences of control, •OH-intervened, and •OH+10-HDA erythrocytes (n=4, $^{**}p < 0.01$). (C) shows the change of dissolved O_2 concentration in the erythrocyte suspension after the administration of 10-HDA (n=6, $^{**}p < 0.01$). (D) displays the dissolved O_2 levels in control, •OH-intervened, and •OH+10-HDA erythrocyte suspensions (n=6, $^{**}p < 0.01$). (E) it is the morphological comparison of control, •OH-intervened, and •OH+10-HDA erythrocytes. (F) compares the MDA productions of the three erythrocyte groups (n=3, $^{*}p < 0.05$, $^{**}p < 0.01$).

of the suspension was significantly heightened in the 10-HDA-treated erythrocytes than that of the CKs ($p < 0.01$) (Figure 1C). Moreover, the level was significantly decreased by •OH ($p < 0.01$) but was significantly restored by 10-HDA ($p < 0.01$) (Figure 1D). Further, erythrocytes supplied by •OH showed the deformed shape. However, with the addition of 10-HDA, the cell shape was recovered (Figure 1E). The significantly elevated MDA level induced by •OH ($p < 0.01$) was also significantly reduced with the addition of 10-HDA ($p < 0.05$) (Figure 1F). Such data indicated that 10-HDA could promote the membrane fluidity and the release of O_2 from erythrocytes, and protect against lipid peroxidation caused by •OH toxicity. In CK and 10-HDA-treated erythrocytes, protein levels of β-actin and EPB41 were not significantly changed ($p > 0.05$, $p > 0.05$) (Figure 2A–C). These protein levels were also not significantly altered by •OH ($p > 0.05$, $p > 0.05$), and not significantly varied with 10-HDA addition ($p > 0.05$, $p > 0.05$) (Figure 2D–F), suggesting that 10-HDA, as well as •OH, may not affect the protein activity in erythrocytes.

10-HDA had the ability to interact with erythrocyte membranous PC and PE

To further elucidate why 10-HDA could ameliorate membrane fluidity, the quantum chemistry methodology was used for calculating the interaction between 10-HDA and PC/PE. The molecules of 10-HDA anion, PC, and PE were optimized and shown in Figure S1. BE values of 10-HDA···PC and 10-HDA···PE dimers were −0.25 eV and −2.52 eV, respectively (Figure 3A), indicating the binding between 10-HDA and PC or PE could occur. The lower BE value and larger bent structure of 10-HDA···PE dimer suggested they may possess a stronger interaction than 10-HDA···PC. Similar to those in ethanol, BE values of 10-HDA···PC and 10-HDA···PE dimers in water environment were −0.31 eV and −2.34 eV, respectively (Figure S2). The bond paths in QTAIM showed that O atom in $-COO^-$ could interact with three H atoms in $-N(CH_3)_3^+$ in 10-HDA···PC, while only one H atom in $-NH_3^+$ in 10-HDA···PE. Moreover, the number of bonding in 10-HDA···PE is much more than that in 10-HDA···PC

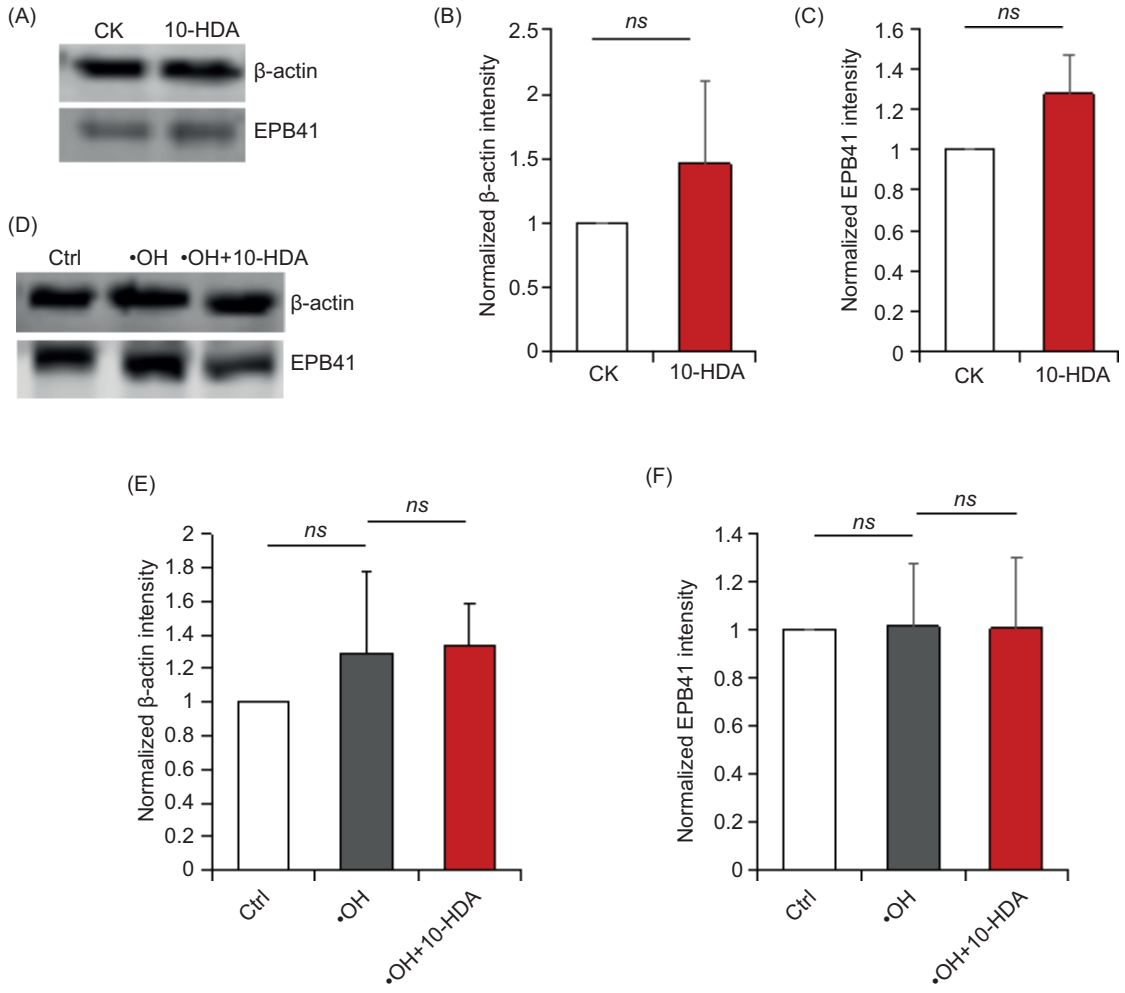

Figure 2. 10-HDA does not change the levels of β-actin and EPB41 in erythrocytes. (A) shows the bands of β-actin and EPB41 of CK and 10-HDA supplemented erythrocytes through Western blotting. (B–C) are the comparisons of their normalized intensities (*n* = 3, *ns*: no significant difference, which means $p > 0.05$). (D) is those of control, •OH-intervened, and •OH + 10-HDA erythrocytes, while (E–F) compare their normalized intensities (*n* = 3, *ns*: no significant difference that $p > 0.05$).

(Figure 3B). Via ELF analysis, almost no regions overlap between 10-HDA anion and PC or PE existed, indicating that the interaction is weak, except for the O atom in -COO^- and the H atom in -NH_3^+ of 10-HDA···PE, which is a bonding region (Figure 3C). In RDG plot, the interaction type between the dimers was the van der Waals interaction. The regions of van der Waals interaction in 10-HDA···PE was much more than that of 10-HDA···PC, and there was no RDG region between the O atom in -COO^- and the H atom in -NH_3^+ in 10-HDA···PE, further revealing it is not a weak interaction (Figure 3D). Altogether, 10-HDA might bind to PC and PE (particularly PE). The HPLC assay showed that the unique peak of 10-HDA (Figure S3A) was visualized in the erythrocyte lysate pre-treated by 10-HDA for either 5 min or 30 min (Figure 4A–B) but no such peak was displayed in erythrocyte sample without 10-HDA addition (Figure S3B). The peak areas to represent the detected 10-HDA amount between erythrocytes of 5 min and 30 min treatment had insignificant difference ($p > 0.05$) (Figure 4C), indicating 10-HDA could quickly target erythrocyte. Via flow cytometry analysis, the intensity of red fluorescence from erythrocytes stained by DiD significantly increased ($p < 0.001$) with the addition of 10-HDA, compared to that of the CKs (Figure 4D–E). The significant enhancement ($p < 0.05$) of the DiD fluorescent intensity was also observed in the 10-HDA-treated erythrocytes using LSCM (Figure 4F–G). In all, 10-HDA could bind to the erythrocyte membrane, which may be contributive to the membrane fluidity.

Discussion

In the present study, we proved that 10-HDA is able to increase the plasma membrane fluidity via the erythrocyte model. Oxidative stress is known to alter the erythrocyte membrane fluidity, which correlates with the

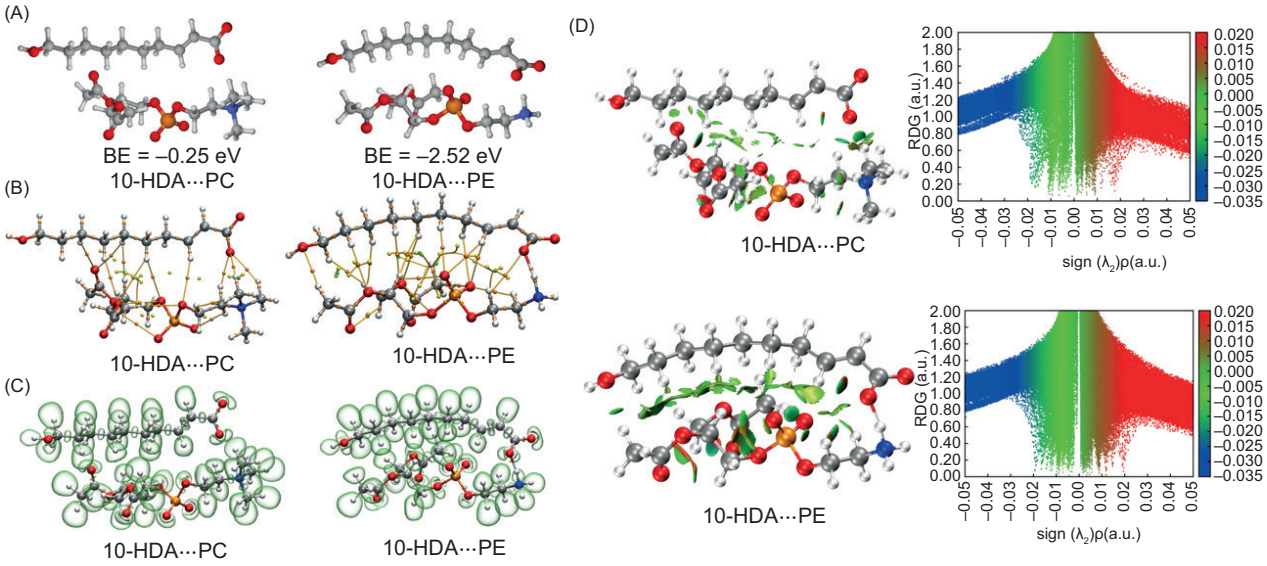

Figure 3. **10-HDA is capable of interacting with erythrocyte membranous PC and PE. (A) shows the optimized geometries for the dimer of 10-HDA···PC and 10-HDA···PE. The white, gray, blue, red, and orange balls denote H, C, N, O, and P atoms, respectively. The BE denotes binding energy (eV). (B) represents the molecular graph for 10-HDA···PC and 10-HDA···PE by QTAIM. The orange, yellow, and green balls are bond, ring, and cage critical points, respectively, and the yellow and orange lines are bond paths. (C) displays the ELF plots for 10-HDA···PC and 10-HDA···PE, respectively. The ELF isovalue is 0.85. The transparent green regions denote the electron localization regions that may be the bonding and lone pairs. (D) includes the RDG plots for 10-HDA···PC and 10-HDA···PE, respectively. The RDG isovalue is 0.05; ρ and sign (λ^2) are electron density and the sign of the second largest eigenvalue of electron density Hessian matrix. All units are a.u.**

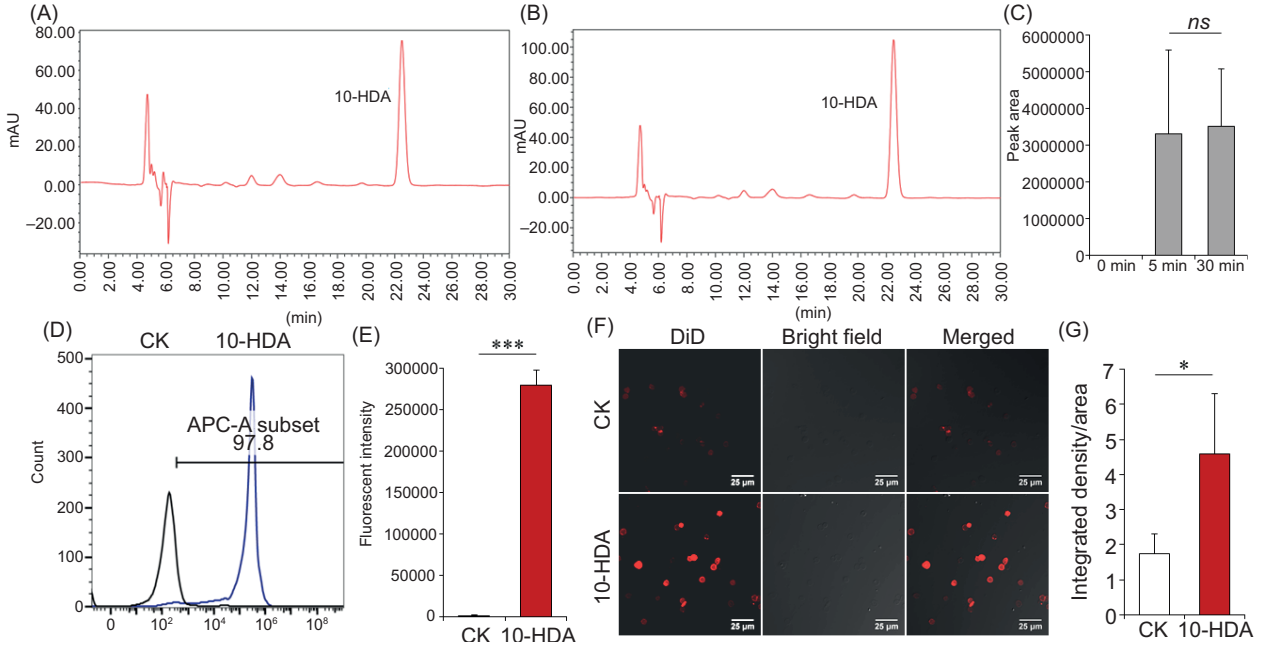

Figure 4. **10-HDA can be incorporated into erythrocyte membrane. (A–B) show the 10-HDA peaks in the HPLC graphs for erythrocyte lysates, in which 10-HDA was pre-added in the erythrocyte suspension for 5 min and 30 min, respectively. The non-specific peak and troughs between 4 min and 8 min might be the interferents from erythrocyte components. (C) is the comparison of 10-HDA peak areas between erythrocytes after 5 min and 30 min treatment by 10-HDA (n = 3, *ns*: no significant difference that $p > 0.05$). (D) is the flow cytometric diagram to represent the difference of fluorescent intensities between CK and 10-HDA treated erythrocytes with DiD staining, which are represented by the black and the blue curves, respectively. (E) shows the fluorescent intensities of the two groups in the flow cytometric analysis (n = 4, ***$p < 0.001$). (F) is the comparison of fluorescent intensities between CK and 10-HDA-treated erythrocytes visualized by LSCM after DiD probing, and (G) compares the integrated density/area values measured by ImageJ software of the two groups (n = 4, *$p < 0.05$).**

progression of a series of diseases. For instance, retinal vein occlusion (RVO) is a vision loss disorder caused by hypoperfusion and hypoxia of the retina. The change of erythrocyte membrane fluidity and whole blood viscosity by oxidative stress is considered the key reason for the pathogenesis of RVO (Becatti *et al.,* 2016). We again proved that 10-HDA is capable of remedying the •OH-induced drop of erythrocyte membrane fluidity. As •OH is non-selective and one of the most potent oxygen free radicals (Richards *et al.,* 2015), 10-HDA has pharmaceutical value in relieving the loss of membrane fluidity under oxidative stress conditions.

Hypoxia is the reduced supply or lack of O_2 in organs, tissues, or cells (Wu and Yotnda 2011). As is the O_2 carrier from lungs to the whole body; erythrocyte dysfunction, such as the case in sickle cell disease, may result in hypoxia (Sun and Xia 2013). There is still the notion that the increase of membrane fluidity reduces the physical barrier to O_2 permeation (Dumas *et al.,* 1997), which suggests that the improvement of erythrocyte membrane fluidity may alleviate the symptom of hypoxia. 10-HDA was found to promote the content of dissolved O_2 in erythrocyte suspension, and to recover the reduced content of dissolved O_2 from the •OH damage. Such fact reflected that 10-HDA may be useful in promoting O_2 release of erythrocytes via regulating the membrane fluidity.

Erythrocyte proteins are pivotal to maintain the cell architecture. Actin composes the cytoskeleton of erythrocytes, and EPB41 strengthens the structure, as well as attaches it to the membrane (Staufenbiel and Lazarides, 1986). Although the proteins are essential for the mechanical properties of erythrocyte such as deformability and stability (Diakowski *et al.,* 2006), the erythrocyte membrane fluidity are believed to be largely reliant on lipid composition rather than proteins (Owen *et al.,* 1982). In the present data, the levels of β-actin and EPB41 in erythrocytes were not affected by 10-HDA, even the cells were treated with •OH and added by 10-HDA, further indicating that 10-HDA interacts with lipids but not proteins to modulate the membrane fluidity and function of erythrocytes.

The fluidity of cell membrane, largely dependent on the unsaturation of fatty acids that compose the lipid bilayer (Upchurch, 2008), can be even triggered by one double bond (-C=C-) (Galván 2018). Moreover, free hydroxyl group (-OH) also determines the membrane fluidity (Sreekanth and Bajaj, 2013). Interestingly, 10-HDA is a -C=C- and -OH bearer. The insertion of 10-HDA into the cell membrane to facilitate the fluidity is reasonable.

Phospholipids are usually the head of the lipid bilayer, in which PC and PE are the major constituents in amount (Schwartz *et al.,* 1985). Some exogenous free fatty acids (for example, docosahexaenoic acid and eicosapentaenoic acid) can interact with the lipid bilayer of the membrane and thus change the cell function (Newell *et al.,* 2017; Dakroub *et al.,* 2021; Fournier *et al.,* 2017). In the framework of DFT in the present study, 10-HDA has potential to bind PC and PE, which helps to unravel the interaction mode of 10-HDA with erythrocyte membrane, and gain insight into the reason for bonding differences between 10-HDA···PC and 10-HDA···PE. Interestingly, the BE values of 10-HDA···PC or 10-HDA···PE are quite similar in both environments of ethanol and water, which are all polar molecules and available for further *ex vivo* and *in vivo* studies. 10-HDA can rapidly interact with erythrocyte, which is attested by the fact that 10-HDA can be detected in erythrocytes 5 min after its addition to the cell suspension. Through DiD staining for erythrocyte membrane, the increased fluorescent intensity by 10-HDA proved it could be part of the membrane. Therefore, interacting with PC and PE of the membrane might be the mechanism for 10-HDA to influence the fluidity.

Conclusion

As is a molecule carrying -C=C- and -OH; 10-HDA is able to increase the membrane fluidity, and to boost the release of O_2 from erythrocytes, which will be useful for improving the membrane fluidity–related diseases, as well as the hypoxia. Such bio-activity of 10-HDA may be profited from its interaction with PC and PE of the membrane. Therefore, our current work would be contributive to the utilization of 10-HDA in nutritional and pharmacological fields. Next, we will seek more evidences about the interaction between 10-HDA and PC/PE in the molecular level, and such effect *in vivo*.

Competing Interests

The authors declare that there is no commercial or financial conflict of interests.

Author's Contributions

The study was designed by Lu Zhang and Pei Fan; the experiments and the data analysis were performed by Fangfang Sha, Peichang Yang, Hui Wang, Junhua Ren, Zirui Li, and Pei Fan; the manuscript was prepared and edited by Fangfang Sha, Lu Zhang, and Pei Fan. All authors contributed to the article and approved the submission.

Funding

This study was funded by the National Natural Science Foundation of China (32070742), and the Innovative

Funds Plan of Henan University of Technology (2021ZKCJ16).

Data Availability Statement

The data in support of the findings of the present work are available from the corresponding author on reasonable request.

References

Ajdžanović V., Jakovljević V., Milenković D., Konić-Ristić A., Živanović J., Jarić I., et al. 2015. Positive effects of naringenin on near-surface membrane fluidity in human erythrocytes. Acta Physiologica Hungarica. 102: 131–136. https://doi.org/10.1556/036.102.2015.2.3

Aozaki S. Decreased membrane fluidity in erythrocytes from patients with Crohn's disease. 1989. Gastroenterologica Japonica. 24: 246–254. https://doi.org/10.1007/BF02774321

Bader RFW. 1990. Atoms in Molecules: A Quantum Theory. Clarendon Press, Oxford, UK. https://doi.org/10.1093/oso/9780198551683.001.0001

Becatti M., Marcucci R., Gori AM., Mannini L., Grifoni E., Alessandrello LA., et al. 2016. Erythrocyte oxidative stress is associated with cell deformability in patients with retinal vein occlusion. Journal of Thrombosis and Haemostasis. 14: 2287–2297. https://doi.org/10.1111/jth.13482

Becke AD and Edgecombe KE. 1990. A simple measure of electron localization in atomic and molecular systems. Journal of Chemical Physics. 92: 5397–5403. https://doi.org/10.1063/1.458517

Becke AD. 1993. Density-functional thermochemistry. III. The role of exact exchange. Journal of Chemical Physics. 98: 5648–5652. https://doi.org/10.1063/1.464913

Chen YF., Wang K., Zhang YZ., Zheng YF., and Hu FL. 2016. In vitro anti-inflammatory effects of three fatty acids from royal jelly. Mediators of Inflammation. 2016: 3583684. https://doi.org/10.1155/2016/3583684

Cooper RA., Durocher JR., and Leslie MH. 1977. Decreased fluidity of red cell membrane lipids in abetalipoproteinemia. Journal of Clinical Investigation. 60: 115–121. https://doi.org/10.1172/JCI108747

Dakroub H., Nowak M., Benoist JF., Noël B., Vedie B., Paul JL., et al. 2021. Eicosapentaenoic acid membrane incorporation stimulates ABCA1-mediated cholesterol efflux from human THP-1 macrophages. Biochimica et Biophysica Acta - Molecular and Cell Biology of Lipids, 1866: 159016. https://doi.org/10.1016/j.bbalip.2021.159016

Diakowski W., Grzybek M., and Sikorski AF. 2006. Protein 4.1, a component of the erythrocyte membrane skeleton and its related homologue proteins forming the protein 4.1/FERM superfamily. Folia Histochemica et Cytobiologica. 44: 231–248.

Dumas D., Muller S., Gouin F., Baros F., Viriot ML., and Stoltz JF. 1997. Membrane fluidity and oxygen diffusion in cholesterol-enriched erythrocyte membrane. Archives of Biochemistry and Biophysics. 341: 34–39. https://doi.org/10.1006/abbi.1997.9936

Fan P., Han B., Hu H., Wei Q., Zhang X., Meng L., et al. 2020. Proteome of thymus and spleen reveals that 10-hydroxydec-2-enoic acid could enhance immunity in mice. Expert Opinion on Therapeutic Targets. 24: 267–279. https://doi.org/10.1080/14728222.2020.1733529

Fan P., Sha F., Ma C., Wei Q., Zhou Y., Shi J., et al. 2022. 10-Hydroxydec-2-enoic acid reduces hydroxyl free radical-induced damage to vascular smooth muscle cells by rescuing protein and energy metabolism. Frontiers in Nutrition. 9: 873892. https://doi.org/10.3389/fnut.2022.873892

Ferretti G., Simonetti O., Offidani AM., Messini L., Cinti B., Marshiseppe I. et al. 1993. Changes of plasma lipids and erythrocyte membrane fluidity in psoriatic children. Pediatric Research. 33: 506–509. https://doi.org/10.1203/00006450-199305000-00017

Filipič B., Gradišnik L., Rihar K., Šooš E., Pereyra A., and Potokar J. 2015. The influence of royal jelly and human interferon-alpha (HuIFN-αN3) on proliferation, glutathione level and lipid peroxidation in human colorectal adenocarcinoma cells in vitro. Arhiv za Higijenu Rada i Toksikologiju. 66: 269–274. https://doi.org/10.1515/aiht-2015-66-2632

Fonseca F., Pénicaud C., Tymczyszyn EE., Gómez-Zavaglia A., and Passot S. 2019. Factors influencing the membrane fluidity and the impact on production of lactic acid bacteria starters. Applied Microbiology and Biotechnology. 103: 6867–6883. https://doi.org/10.1007/s00253-019-10002-1

Fournier N., Sayet G., Vedie B., Nowak M., Allaoui F., Solgadi A., et al. 2017. Eicosapentaenoic acid membrane incorporation impairs cholesterol efflux from cholesterol-loaded human macrophages by reducing the cholesteryl ester mobilization from lipid droplets. Biochimica et Biophysica Acta - Molecular and Cell Biology of Lipids. 1862: 1079–1091. https://doi.org/10.1016/j.bbalip.2017.07.011

Fratini F., Cilia C., Mancini S., and Felicioli A. 2016. Royal jelly: an ancient remedy with remarkable antibacteria properties. Microbiological Research. 192: 130–141. https://doi.org/10.1016/j.micres.2016.06.007

Galván I. 2018. Evidence of evolutionary optimization of fatty acid length and unsaturation. Journal of Evolutionary Biology. 31: 172–176. https://doi.org/10.1111/jeb.13198

Grimme S., Ehrlich S., and Goerigk L. 2011. Effect of the damping function in dispersion corrected density functional theory. Journal of Computational Chemistry. 32: 1456–1465. https://doi.org/10.1002/jcc.21759

Humphrey W., Dalke A., and Schulten K. 1996. VMD: visual molecular dynamics. Journal of Molecular Graphics. 14: 33–38. https://doi.org/10.1016/0263-7855(96)00018-5

Johnson ER., Keinan S., Mori-Sánchez P., Contreras-García J., Cohen AJ., and Yang W. 2010. Revealing noncovalent interactions. Journal of the American Chemical Society. 132: 6498–6506. https://doi.org/10.1021/ja100936w

Lee C., Yang W., and Parr RG. 1988. Development of the Colle-Salvetti correlation-energy formula into a functional of the electron density. Physical Review B: Condensed Matter and Materials Physics. 37: 785–789. https://doi.org/10.1103/PhysRevB.37.785

Lu T., and Chen F. 2012. Multiwfn: a multifunctional wavefunction analyzer. Journal of Computational Chemistry. 33: 580–592. https://doi.org/10.1002/jcc.22885

Marenich AV., Cramer CJ., and Truhlar DG. 2009. Universal solvation model based on solute electron density and on a continuum model of the solvent defined by the bulk dielectric constant and atomic surface tensions. Journal of Physical Chemistry B. 113: 6378–6396. https://doi.org/10.1021/jp810292n

Newell M., Baker K., Postovit LM., and Field CJ. 2017. A critical review on the effect of docosahexaenoic acid (DHA) on cancer cell cycle progression. International Journal of Molecular Sciences. 18: 1784. https://doi.org/10.3390/ijms18081784

Owen JS., Bruckdorfer KR., Day RC., and McIntyre N. 1982. Decreased erythrocyte membrane fluidity and altered lipid composition in human liver disease. Journal of Lipid Research. 23: 124–132. https://doi.org/10.1016/S0022-2275(20)38181-5

Richards SL., Wilkins KA., Swarbreck SM., Anderson AA., Habib N., Smith AG., et al. 2015. The hydroxyl radical in plants: from seed to seed. Journal of Experimental Botany. 66: 37–46. https://doi.org/10.1093/jxb/eru398

Schwartz RS., Chiu DT., and Lubin B. 1985. Plasma membrane phospholipid organization in human erythrocytes. Current Topics in Hematology. 5: 63–112.

Shin S., Ku Y., Babu N., and Singh M. 2007. Erythrocyte deformability and its variation in diabetes mellitus. Indian Journal of Experiemental Biology. 45: 121–128.

Sreekanth V., and Bajaj A. 2013. Number of free hydroxyl groups on bile acid phospholipids determines the fluidity and hydration of model membranes. Journal of Physical Chemistry B. 117: 12135–12144. https://doi.org/10.1021/jp406340y

Startek JB., Milici A., Naert R., Segal A., Alpizar YA., Voets T., et al. 2021. The agonist action of alkylphenols on TRPA1 relates to their effects on membrane lipid order: implications for TRPA1-mediated chemosensation. International Journal of Molecular Sciences. 22: 3368. https://doi.org/10.3390/ijms22073368

Staufenbiel M., and Lazarides E. 1986. Assembly of protein 4.1 during chicken erythroid differentiation. Journal of Cell Biology. 102: 1157–1163. https://doi.org/10.1083/jcb.102.4.1157

Sun K., and Xia Y. 2013. New insights into sickle cell disease: a disease of hypoxia. Current Opinion in Hematology. 20: 215–221. https://doi.org/10.1097/MOH.0b013e32835f55f9

Tsuda K., Kinoshita Y., Nishio I., and Masuyama Y. 2001. Hyperinsulinemia is a determinant of membrane fluidity of erythrocytes in essential hypertension. American Journal of Hypertension. 14: 419–423. https://doi.org/10.1016/S0895-7061(00)01247-4

Upchurch RG. 2008. Fatty acid unsaturation, mobilization, and regulation in the response of plants to stress. Biotechnology Letters. 30: 967–977. https://doi.org/10.1007/s10529-008-9639-z

Watanabe H., Kobayashi A., Yamamoto T., Suzuki S., Hayashi H., and Yamazaki N. 1990. Alterations of human erythrocyte membrane fluidity by oxygen-derived free radicals and calcium. Free Radical Biology & Medicine. 8: 507–514. https://doi.org/10.1016/0891-5849(90)90150-H

Weigend F. 2006. Accurate coulomb-fitting basis sets for H to Rn. Physical Chemistry Chemical Physics. 8: 1057–1065. https://doi.org/10.1039/b515623h

Wu D., and Yotnda P. 2011. Induction and testing of hypoxia in cell culture. Journal of Visualized Experiments, 2899. https://doi.org/10.3791/2899-v

Yang W., Tian Y., Han M., and Miao X. 2017. Longevity extension of worker honey bees (Apis mellifera) by royal jelly: optimal dose and active ingredient. PeerJ. 5: e3118. https://doi.org/10.7717/peerj.3118

Yang YC., Chou WM., Widowati DA., Lin IP., and Peng CC. 2018. 10-hydroxy-2-decenoic acid of royal jelly exhibits bactericide and anti-inflammatory activity in human colon cancer cells. BMC Complementary and Alternative Medicine. 18: 202. https://doi.org/10.1186/s12906-018-2267-9

You M., Miao Z., Pan Y., and Hu F. 2019. Trans-10-hydroxy-2-decenoic acid alleviates LPS-induced blood-brain barrier dysfunction by activating the AMPK/PI3K/AKT pathway. European Journal of Pharmacology. 865: 172736. https://doi.org/10.1016/j.ejphar.2019.172736

You M., Miao Z., Tian J., and Hu F. 2020. Trans-10-hydroxy-2-decenoic acid protects against LPS-induced neuroinflammation through FOXO1-mediated activation of autophagy. European Journal of Nutrition. 59: 2875–2892. https://doi.org/10.1007/s00394-019-02128-9

Zheng J., Lai W., Zhu G., Wan M., Chen J., Tai Y., et al. 2013. 10-Hydroxy-2-decenoic acid prevents ultraviolet A-induced damage and matrix metalloproteinases expression in human dermal fibroblasts. Journal of the European Academy of Dermatology and Venereology. 27: 1269–1277. https://doi.org/10.1111/j.1468-3083.2012.04707.x

Supplementary

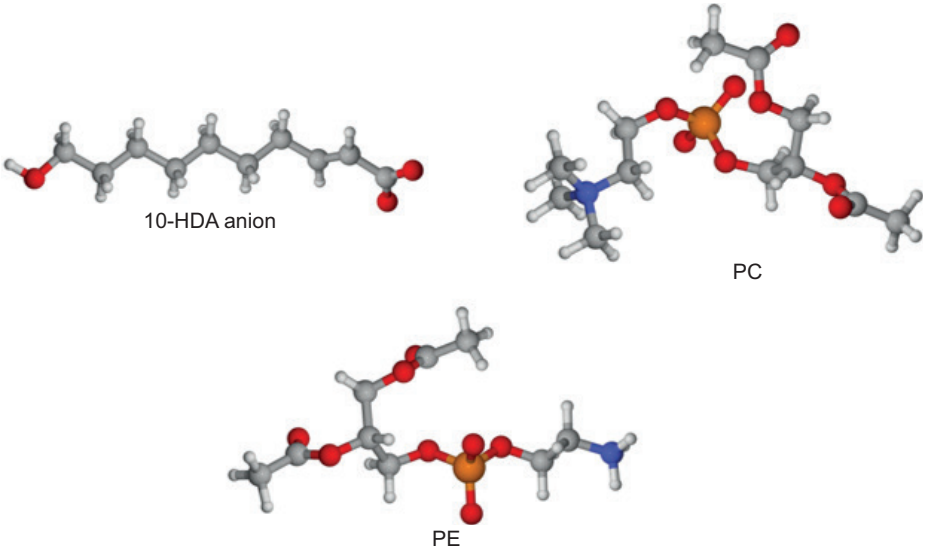

Figure S1. The optimized geometries for the 10-HDA anion, PC, and PE. The white, gray, blue, red, and orange balls represent the atoms of H, C, N, O, and P, respectively.

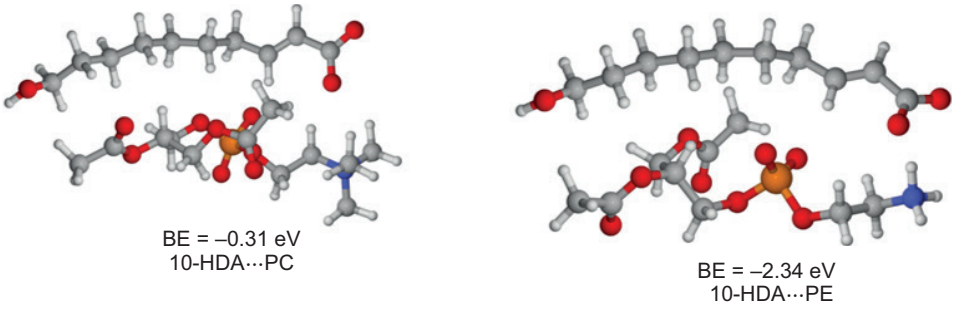

Figure S2. The BE values of 10-HDA···PC and 10-HDA···PE in water environment. The white, gray, blue, red, and orange balls denote H, C, N, O, and P atoms, respectively.

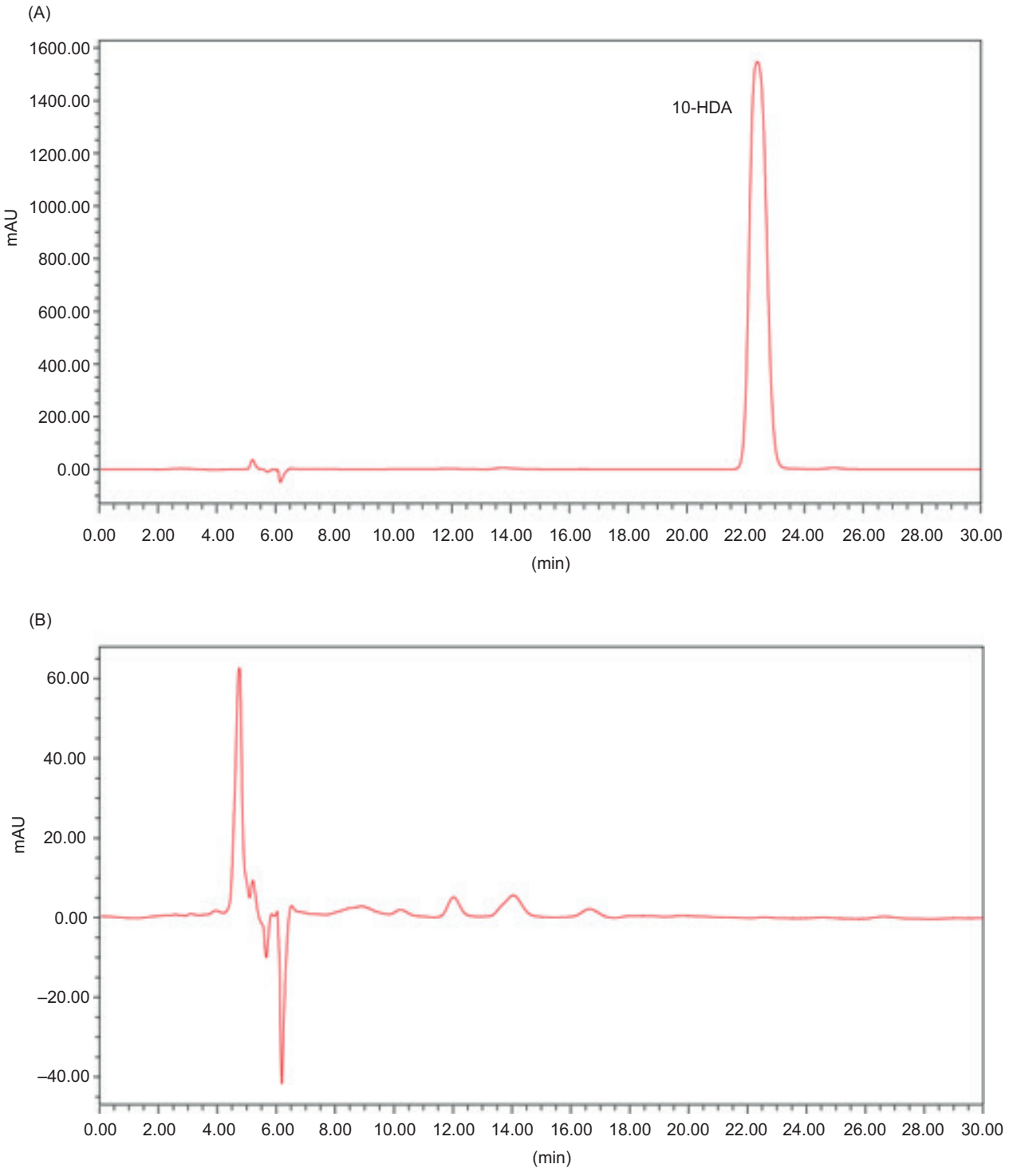

Figure S3. The HPLC assay for 10-HDA in 10-HDA solution and erythrocyte lysate without 10-HDA addition. (A) is the HPLC graph for the 10-HDA solution. (B) is the HPLC graph for the erythrocyte lysate in which the 10-HDA is not added.